Original Article

Ultrasound biomicroscopy image patterns in normal upper eyelid and congenital ptosis in the Indian population

Abhidnya Surve, Rachna Meel, Neelam Pushker, M S Bajaj

Purpose: To study the features of upper eyelid in healthy individual and different types of congenital ptosis in the Indian population using ultrasound biomicroscopy (UBM). **Methods:** This was a prospective observational study at a tertiary care center. Eyelid structure of healthy individuals with no eyelid abnormalities ($n = 19$); simple congenital ptosis ($n = 33$) cases; Marcus Gunn jaw-winking ptosis (MGJWP, $n = 7$) cases, and blepharophimosis-ptosis-epicanthus inversus syndrome (BPES, $n = 20$) cases were studied on a vertical UBM scan using 50-MHz probe. Lid-thickness, tarsal-thickness, orbicularis oculi and levator-Muller-orbital septum-conjunctival (LMSC) complex were measured in primary gaze. Comparison was made between four groups and results were statistically analyzed using ANOVA test. In normal individuals, LMSC measurements were repeated in down-gaze imaging. **Results:** Skin with subcutaneous tissue, LMSC complex and pre-aponeurotic fat-pad appeared echodense while orbicularis oculi and tarsus appeared echolucent. In primary gaze, mean thickness (± standard deviation) of the eyelid, tarsus, orbicularis oculi and LMSC, respectively, were: 1.612 ± 0.205, 0.907 ± 0.098, 0.336 ± 0.083, and 0.785 ± 0.135 mm in normal individual. LMSC showed 46.64% increase in thickness on down-gaze. The mean eyelid thickness and LMSC were thicker in MGJWP and BPES as compared to normal. In different types of congenital ptosis cases, various patterns of UBM imaging were observed. **Conclusion:** UBM allows noninvasive imaging of eyelid structures with good anatomical correspondence in normal eyelids and study the structural alterations of eyelids in different types of congenital ptosis. UBM can be used to highlight the anatomical difference in normal eyelids that may help modify the surgery for better cosmetic outcomes. Furthermore, it has the potential to be used in preoperative evaluation and operative planning in certain types of acquired ptosis, which needs to be evaluated.

Key words: Asian, congenital ptosis, levator-Muller complex, normal upper eyelid, ultrasound biomicroscopy

Ultrasound biomicroscopy (UBM) is a real-time noninvasive imaging technique with high resolution. It is a high-frequency ultrasonography technique that employs 35–100 MHz frequency and provides a resolution of 25 µm to 50 µm with a depth of penetration up to 4 mm.[1,2] UBM is being widely explored in the area of ophthalmology since its inception. It has been used for imaging of various structures including cornea, sclera, anterior chamber angle, iris, ciliary body, lens, intraocular lens placement, eyelid lesions and lacrimal drainage system.[3-6] It has also been used for functional assessment in accommodative response, blinking mechanism effect on the lacrimal system and dynamic changes in the lower eyelid.[7-9] Studies have shown that UBM features have correlated well with the histopathological features in terms of depth and tissue characterization in eyelid lesions.[4,5] A few studies have delineated the eyelid morphology using UBM in normal and ptosis patients.[9-13] However, no studies in the literature have outlined the various changes in different subtypes of congenital blepharoptosis using UBM.

Eyelids are seen to have inter-racial differences which form a major role in individual appearance. These differences are imperative to be considered during eyelid surgeries to obtain optimal results and maintain individual ethnic characteristic. In Asian population, eyelids are divided into various types and subtypes according to the lid crease and epicanthal fold. Many differences with their surgical implications are being lately identified and studied using various techniques, especially in the Asian eyelid.[13-17] Prior studies have utilized MRI with an ultrafine surface coil to image the eyelid structures including levator aponeurosis.[18,19] However, UBM allows easy, time-saving, cost-effective, noninvasive and high-resolution imaging of upper eyelid allowing preoperative assessment of various structures of the eyelid.

Herein, we have studied the UBM imaging of upper eyelid in the normal Asian population and in various types of congenital ptosis including simple congenital ptosis (SCP), Marcus Gunn jaw-winking ptosis (MGJWP), and blepharophimosis-ptosis-epicanthus inversus syndrome (BPES).

Dr. R. P. Centre for Ophthalmic Sciences, All India Institute of Medical Sciences, New Delhi, India

Correspondence to: Dr. Rachna Meel, Dr. R. P. Centre for Ophthalmic Sciences, All India Institute of Medical Sciences, Ansari Nagar, New Delhi, India. E-mail: dr.rachnameel@gmail.com

Cite this article as: Surve A, Meel R, Pushker N, Bajaj MS. Ultrasound biomicroscopy image patterns in normal upper eyelid and congenital ptosis in the Indian population. Indian J Ophthalmol 2018;66:383-8.

Methods

This was a prospective observational study conducted at a tertiary care eye center in India. Institutional Ethics Committee approval was obtained and informed consent was taken in accordance with the principles of Declaration of Helsinki. A healthy individual with no eyelid abnormalities attending out-patient department and cases of congenital moderate to severe grade ptosis admitted for surgery over the period of May 2015 – August 2016 were recruited. Cases with a history of previous eyelid surgery or presence of ocular surface disease were excluded from the study. After complete systemic and ophthalmic examination, patients with systemic disorders such as myasthenia, thyroid illness or muscular disorders were excluded from the study.

The upper eyelid was imaged using an UBM scanner (SONOMED VuMax II UBM, New York, USA) with a 50-MHz transducer probe and a scleral cup filled with normal saline. All imaging and measurements were carried out by a single operator to avoid any inter-observer variation. The patient was placed in supine position and the eyelid to be imaged was closed with other eye open and fixating at the ceiling to maintain primary position. A scleral cup was placed at the center of the closed upper eyelid, just above the eyelash border and filled with normal saline as a coupling agent. Images were taken from the vertical scan passing through the center of the cornea which was indicated by a sharp and central corneal image on the scan. All imaging were repeated thrice and the characteristics of eyelid structures including echotexture and echogenicity were noted. No color coding was used for delineation of different layers of the eyelid. Wherever possible, the thickness of tarsus was measured at a point midway between upper and lower tarsal border. Eyelid thickness, orbicularis the average was noted. and levator-Muller orbital septum conjunctival complex (LMSC) were measured just above the upper border of tarsus. LMSC was measured as a single unit because it was difficult to distinguish between the different component layers precisely on UBM. In a normal individual, the LMSC was again measured at the upper tarsal edge with the patient fixing in down-gaze with the opposite eye.

Minimum three measurements were recorded for each parameter and the average was noted. The mean and the standard deviation were calculated for each parameter in all groups and the data were compared using ANOVA and *t*-test. Data were analyzed using SPSS Statistical Software (SPSS Inc., version 16, Chicago, IL, USA) and the value of $P < 0.05$ was considered as statistically significant.

Results

Seventy-nine Indian eyelids were analyzed using UBM, which included 19 normal eyelids, 33 with SCP, 7 with MGJWP and 20 with BPES. MGJWP cases had predominantly moderate degree while SCP and BPES cases had a predominantly severe degree of ptosis. The demography and clinical parameters are summarized in Table 1.

In normal individuals, the vertical scan of UBM imaging of upper eyelid showed skin and subcutaneous tissue as the anteriormost echodense layer. Orbicularis oculi was seen as a homogenously echolucent layer just beneath them extending throughout the length of the eyelid. Tarsus was seen as a well-defined echolucent structure. Within the echolucent tarsus, an echodense racemose pattern was identified which could be explained by lipid-filled meibomian glands in the tarsus. The preaponeurotic fat pad was identified as an echodense well-defined ellipsoid structure toward the superior edge of the scan. The echodense structure between the tarsus and orbicularis oculi is the levator palpebrae superioris (LPS) aponeurosis and septum that insert on the anterior surface of the tarsus. On dynamic imaging, few fibers from the aponeurosis were seen passing obliquely to the orbicularis and surface of eyelid suggestive of the skin attachments in most of the cases [Fig. 1a]. At the upper edge of the tarsus, an echodense layered structure was seen between the orbicularis oculi and posterior border of the eyelid, which was termed the LMSC complex and measurement was taken at this location [Table 1]. It was not possible to measure orbital septum, LPS aponeurosis and Muller's muscle separately, as it was difficult to identify these structures separately at this location [Figs. 1a and 2a]. In down-gaze, echodense sclera was prominently seen with similar appearance of other structures [Fig. 1b]. LMSC was significantly thicker in down-gaze with a mean ± SD of 1.089 ± 0.121 ($P < 0.01$).

Various changes were seen in different types of congenital ptosis. In SCP cases, three variations in the imaging of UBM

Table 1: Demography, clinical parameters, and ultrasound biomicroscopy measurements

	Normal	SCP	MGJWP	BPES
Number of eyelids (*n*)	19	33	7	20
Age (mean±SD)	24.79±6.98	12.49±6.87	14.29±7.83	13.7±6.49
Males	15	23	5	8
Severe ptosis (%)	-	30 (90.91)	3 (42.86)	18 (90.0)
LPS action <4 mm (%)	-	29 (87.88)	3 (42.86)	19 (95.0)
LFP	0	5	3	13
Eyelid thickness (mean±SD)	1.612±0.205	1.75±0.504	2.138±0.453	2.301±0.459
Tarsal thickness (mean±SD)	0.907±0.098	0.819±0.134	0.85±0.1	0.68±0.115 (8)[†]
Orbicularis oculi (mean±SD)	0.336±0.083	0.341±0.164 (31)[†]	0.299±0.057	0.431±0.269 (8)[†]
LMSC complex (mean±SD)	0.785±0.135	0.848±0.298 (31)[†]	1.014±0.338	1.008±0.366 (6)[†]

[†]Number of individuals where measurable. SCP: Simple congenital ptosis, MGJWP: Marcus Gunn jaw winking ptosis, BPES: Blepharophimosis-ptosis-epicanthus inversus syndrome, LPS: Levator Palpebrae Superioris, LMSC: Levator-Muller-septal-conjunctival complex, LFP: Low fat pad, SD: Standard deviation
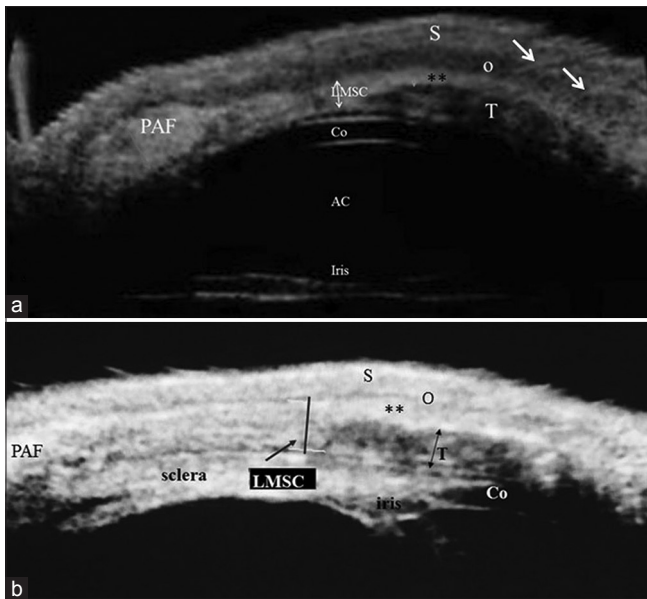
Figure 1: Vertical ultrasound biomicroscopy scan of upper eyelid of normal individual in primary gaze (a) and down-gaze (b) through the centre of cornea (Co). S: Skin and subcutaneous tissue, O: Orbicularis oculi, T: Tarsus, (**): Levator aponeurosis, LMSC: Levator-Muller-septal-conjunctival complex; PAF: Preaponeurotic fat-pad. Few aponeurotic fibers (arrows) seen extending from LMSC to skin

Figure 2: Ultrasound biomicroscopy imaging pattern in SCP: A 9-year-old-female OD no ptosis (a) and OS severe-grade SCP (b). OS: thicker eyelid and low lying preaponeurotic fat-pad (F) extending up to anterior surface of tarsus (*); 6-year-old-female, severe-grade SCP (c) prominent LMSC complex (L) and preaponeurotic fat-pad (F); 26-year-old-male, moderate-grade SCP (d) thinner eyelid with the absence of fat-pad. SCP: Simple congenital ptosis, OD: Right eye, OS: Left eye, LMSC: Levator-Muller-septal-conjunctival complex

of upper eyelid were seen [Fig. 2b-d]. One pattern showed the varying level of preaponeurotic fat pad in relation to eyelid structures with possible recognition of various layers of the eyelid. In another pattern, seen in five cases, an echodense large low-lying fat pad was seen extending over the tarsus which made delineation of various eyelid structures difficult. In the third pattern, thin eyelid with no fat pad was seen in three cases. Cases with SCP had thicker eyelid and thinner tarsus as compared to normal, but the difference was not statistically significant [Table 1]. Overall, in congenitally ptosis group, SCP had the thinnest eyelid as compared to others with a $P < 0.001$.

In MGJWP cases, UBM showed thicker eyelids as compared to normal individuals with a *P* value of 0.046 [Table 1]. Three (42.86%) cases had a low-fat pad which made delineation of eyelid structures difficult [Fig. 3a-c]. In BPES cases, UBM showed echolucent tarsus with increased hyperechogenicity throughout the remaining part of the eyelid. Thus, delineation of various eyelid components was difficult [Fig. 4a-c]. Furthermore, low-fat pad extending over tarsus was seen in 13 (65%) cases. However, eyelid structures were differentiable in six cases. Thicker eyelids and thinner tarsus were seen in BPES, respectively, as compared to normal ($P < 0.001$, <0.001), SCP ($P < 0.001$, 0.027) and MGJWP cases ($P = 1.00$, 0.046).

Discussion

Eyelid is a complex structure with varied anatomical differences between different races. Various studies have highlighted the anatomical variation in the diverse Asian population and its surgical implications[13-17] Different pathologies involving eyelid range from simple inclusion cyst, chalazion, traumatic laceration, ptosis and blepharochalasis to multiple benign and malignant tumors. Various surgeries are performed to treat
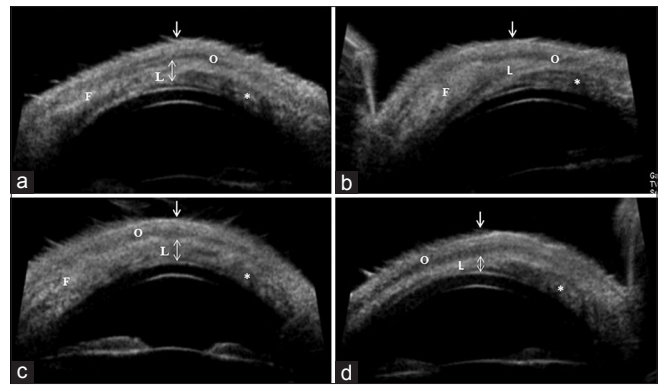
different conditions and correct the abnormalities due to its sequelae. Knowledge of the eyelid anatomy and numerous differences between various individual is thus crucial to achieve the optimal surgical outcome and maintain the ethnical characteristic of an individual. With the recent improvement in technology, UBM could provide a noninvasive, cost-effective alternative to study the eyelid anatomy in different individual and the changes occurring in various pathologies with enhanced resolution. It has been used to study various eyelid lesions and its correlation with histological characteristics.[3-5] However, a few studies have evaluated the upper eyelid structure in normal and ptotic individuals using UBM in the past.[10-12] Recent studies have documented dynamic imaging of fat pad in lower eyelids and the anatomical difference in various races using UBM.[9,13] This anatomical knowledge would certainly translate into meticulous surgery with fine esthetic outcome.

In this study, we found that almost all the eyelid structures could be reliably identified on UBM with good anatomical correlation. The tarsal plate, which is composed of fibro-collagenous connective tissue, appeared echolucent with lipid-filled meibomian glands appreciated as an echodense racemose pattern within the echolucent tarsus. Tarsus, being a rigid structure, was used as a landmark for measurement of pliable tissue such as LPS, orbicularis and eyelid thickness. Normally extra-ocular muscle is seen to have low echogenicity on orbital ultrasonography, and any replacement of muscle tissue with fat and fibrous tissue causes an increase in muscle echogenicity as seen in cases of thyroid-associated ophthalmopathy, attributing to increase in the number of sound reflections from within the muscle.[20] In this study, orbicularis oculi muscle was seen as a uniform echo-lucent band just beneath the echodense skin and subcutaneous tissue throughout the length of the eyelid on UBM. The orbital septum is a thin fibrous multilayered membrane originating at the arcus marginalis and is considered to be a continuation of the orbital fascial system with distal mergence into the anterior surface of levator aponeurosis. The septum along with levator aponeurosis inserts on the superior and anterior surface of tarsus at a varying location with few fibers running forward
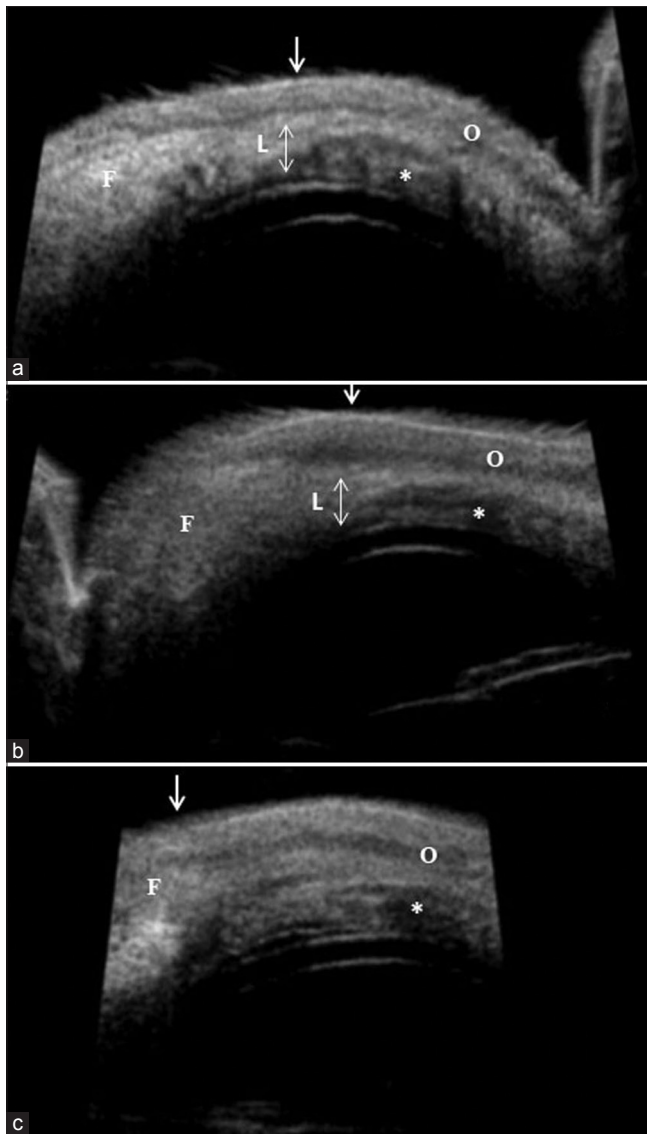
Figure 3: Ultrasound biomicroscopy imaging pattern in Marcus Gunn jaw winking ptosis. (a) Thicker eyelid (arrow), tarsus (*) and LMSC (L) with prominent fat-pad (F). (b) Fat pad approaching near the upper border of tarsus. (c) Prominent low-fat pad extending to the anterior border of tarsus making delineation of LMSC difficult. LMSC: Levator-Muller-septal-conjunctival complex

Figure 4: Ultrasound biomicroscopy imaging in blepharophimosis-ptosis-epicanthus-inversus syndrome. (a and b) 15-year-old-female, 5-year-old-male respectively shows thicker eyelids with hypo-echoic tarsus (*) with increased hyper-echogenecity throughout the remaining part of the eyelid. (c) 20-year-old-female showing various eyelid structures with thick eyelids (arrow) and thinner tarsus (*). LMSC (L) and preaponeurotic fat-pad (F) could be delineated. LMSC: Levator-Muller-septal-conjunctival complex

and downward to insert onto the inter-fascicular septae of the pretarsal orbicularis muscle, subcutaneous tissue and skin.[15,16,21] This complex of levator aponeurosis and orbital septum, being fibrous tissue was imaged as an echodense structure anterior to the tarsus. At the upper border of Tarsus, Muller's muscle and conjunctiva could not be identified separately from levator aponeurosis and orbital septum. Thus, in our study, the LMSC complex was measured as a single echodense structure between echolucent orbicularis and the posterior border of the eyelid. On dynamic UBM, echodense septae were seen arising from this structure extending to the skin and subcutaneous tissue [Fig. 1a].

Previous studies have not mentioned about the fat pad in the upper eyelid, which was very well identified in our study.[10-13] The pre-aponeurotic fat pad was seen as an ellipsoid echodense
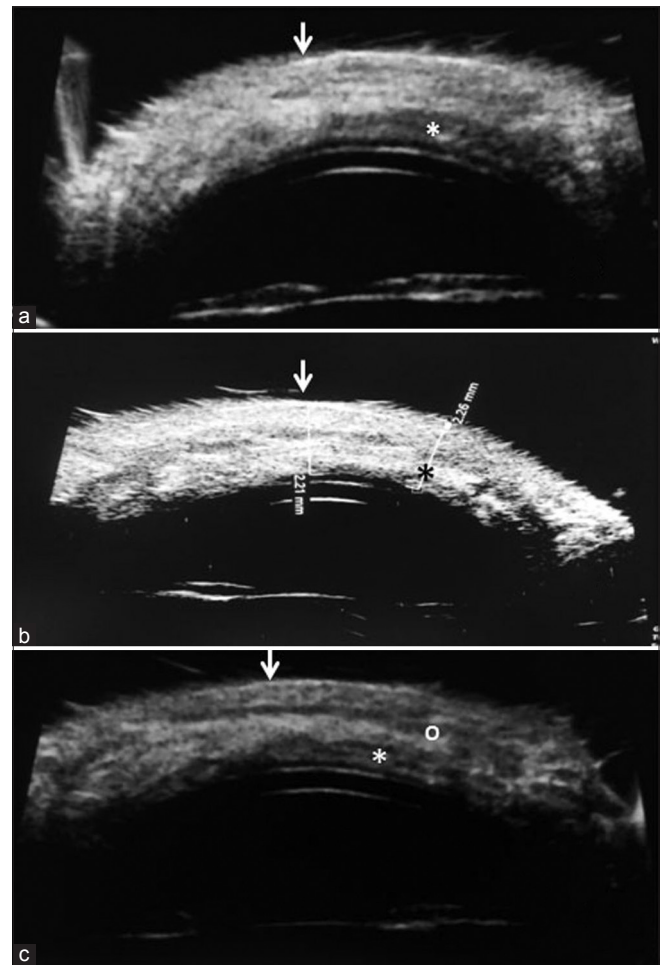
structure at the upper edge of the scan between the septum and LPS aponeurosis in most of the Indian eyelids as contrary to the presence of submuscularis or preseptal fat pad in most of the other Asian population.[15,17] In few cases, an echolucent structure was seen behind this fat pad which was probably the levator muscle. This highlights the further diversity of the eyelid anatomy in the Asian population and also the role of UBM in addition to other anatomical, histological studies to study these features.

Histologically, thickness of eyelid, tarsus,[22] Muller muscle,[23] and superior and inferior branch of levator aponeurosis[24] is reported as approximately 1.5–2.0 mm, 1.00 mm, 0.10 ± 0.03 mm, 0.2–0.55 mm (0.340) and 0.13–0.42 mm (0.248), respectively. These correlated with the measurements observed on UBM imaging in normal eyelids [Table 1]. The LMSC complex containing levator aponeurosis, Muller muscle, septum and conjunctiva was as expected thicker (0.785 ± 0.135 mm) than the individual component. In down-gaze, this thickness increased to 1.089 ± 0.121 mm [Fig. 2b]. On up-gaze with

the closed eyelid, there is contraction of the LPS muscle with stretch of the aponeurosis which should result in an increase in muscle thickness and a decrease in the aponeurosis thickness. Similarly, on down-gaze, there is relaxation of the muscle leading to decrease in muscle thickness and increase in aponeurosis thickness. This was confirmed in the study, where we found 46.64% increase in LMSC thickness on down-gaze in normal eyelids ($P < 0.01$). No significant correlation was seen between the structural variation on UBM and severity of ptosis (determined by LPS action and amount of ptosis). However, this was limited by the small number of cases with a higher proportion of cases being severe ptosis in each subgroup.

Ptosis surgery requires meticulous dissection of different layers of the eyelid to avoid irregular scarring and to form the normal contour and architecture of the eyelid according to a person's esthetics. Fat pad forms an important component of the eyelid and variations are known in its distribution.[14,15,17] Intraoperatively, it allows identification of the pre-aponeurotic plane while excess fat can cause difficulty during surgery. This fat pad was seen at various levels on UBM imaging in cases of ptosis. This probably corresponded to the junctional anatomy of the septum, levator aponeurosis and tarsus.[14-16,24] UBM of SCP cases showed a pattern similar to normal individuals and varying level of fat pad in most of the cases. UBM of the eyelid in MGJWP cases showed comparatively thicker eyelids, and the low fat pad was seen in three cases. MGJWP is considered as a neurogenic type of ptosis with abnormally innervated hypertrophied muscle fibers and atrophic fibers associated with fibro-fatty infiltration, which could be responsible for the increased thickness of the LMSC and hence, of the eyelids.[25] BPES cases are known to have maldeveloped short eyelids with fibro-fatty infiltration which can also lead to the difficult intraoperative delineation of the eyelid structures.[26] On UBM also, eyelids in most of the BPES cases showed an altered pattern with echolucent tarsus and increased echogenicity in the remaining part of the eyelid making demarcation of various eyelid structures difficult. LMSC, orbicularis oculi and eyelids were found to be significantly thicker as compared to normal and SCP cases, probably due to fibro-fatty infiltration and short eyelids in BPES. However, the tarsus was significantly thinner in this group. Thus, UBM imaging showed various patterns indicative of the structural alteration in upper eyelid in congenital ptosis.

This knowledge of eyelid anatomy and changes in various types of ptosis using UBM technique may further be used for preoperative assessment, planning and improving surgical outcomes in eyelid surgeries. Furthermore, further exploration of its potential use in preoperative assessment in acquired ptosis due to post-traumatic or senile LPS aponeurotic dehiscence or disinsertion is needed. UBM may help detect and grade the degree of dehiscence and thus planning of surgery, possibly making surgical outcomes more predictable. However, this needs to be assessed in further studies.

There are a few limitations of this study including the smaller number of cases. First, the age distribution between the normal individual group and the ptotic group was different. However, prior studies have shown no difference with age and gender.[10] Second, eyelids being a pliable structure, the use of scleral cup for UBM may cause intra and inter-observer variations in the measurements leading to less repeatability.

However, in our study, the measurements were done by a single observer and at the upper border of Tarsus. Tarsus being a rigid structure would thus decrease the variation due to the pliability of the eyelid. However, intra-observer variation cannot be avoided, and thus, an average of three readings was taken for each parameter. Third, UBM being designed for anterior segment imaging, the speed of sound in eyelid tissue is different from the preset value. With advancement in technology and increased resolution, this limitation may soon be overcome.

Conclusion

Our study showed that various eyelid structures can be definitely identified separately on UBM with a good correlation with the anatomy of the eyelid that varies with different types of congenital ptosis. Thus, UBM allows noninvasive, cost-effective, time-saving alternative for imaging different eyelid structures, studying anatomical variations in different races and individuals and potential use in preoperative assessment in certain types of ptosis, which needs further exploration.

Conflicts of interest
There are no conflicts of interest.

References

1. Pavlin CJ, Harasiewicz K, Sherar MD, Foster FS. Clinical use of ultrasound biomicroscopy. Ophthalmology 1991;98:287-95.

2. Foster FS, Pavlin CJ, Harasiewicz KA, Christopher DA, Turnbull DH. Advances in ultrasound biomicroscopy. Ultrasound Med Biol 2000;26:1-27.

3. Silverman RH. High-resolution ultrasound imaging of the eye – A review. Clin Exp Ophthalmol 2009;37:54-67.

4. Kikkawa DO, Ochabski R, Weinreb RN. Ultrasound biomicroscopy of eyelid lesions. Ophthalmologica 2003;217:20-3.

5. Bajaj MS, Aalok L, Gupta V, Sen S, Pushker N, Chandra M, *et al.* Ultrasound biomicroscopic appearances of eyelid lesions at 50 MHz. J Clin Ultrasound 2007;35:424-9.

6. Al-Faky YH. Anatomical utility of ultrasound biomicroscopy in the lacrimal drainage system. Br J Ophthalmol 2011;95:1446-50.

7. Ramasubramanian V, Glasser A. Prediction of accommodative optical response in prepresbyopic patients using ultrasound biomicroscopy. J Cataract Refract Surg 2015;41:964-80.

8. Pavlidis M, Stupp T, Grenzebach U, Busse H, Thanos S. Ultrasonic visualization of the effect of blinking on the lacrimal pump mechanism. Graefes Arch Clin Exp Ophthalmol 2005;243:228-34.

9. Rajabi MT, Papageorgiou K, Chang SH, Jarullazada I, Taban M, Hwang CJ, *et al.* Ultrasonographic visualization of lower eyelid structures and dynamic motion analysis. Int J Ophthalmol 2013;6:592-5.

10. Demirci H, Nelson CC. Ultrasound biomicroscopy of the upper eyelid structures in normal eyelids. Ophthal Plast Reconstr Surg 2007;23:122-5.

11. Hosal BM, Pavlin CJ, Hurwitz JJ. Clinical use of ultrasound biomicroscopy in involutional blepharoptosis. Orbit 1994;13:167-71.

12. Hoşal BM, Ayer NG, Zilelioğlu G, Elhan AH. Ultrasound biomicroscopy of the levator aponeurosis in congenital and aponeurotic blepharoptosis. Ophthal Plast Reconstr Surg 2004;20:308-11.

13. Saonanon P, Thongtong P, Wongwuticomjon T. Differences between single and double eyelid anatomy in Asians using ultrasound biomicroscopy. Asia Pac J Ophthalmol (Phila) 2016;5:335-8.

14. Kiranantawat K, Suhk JH, Nguyen AH. The Asian eyelid: Relevant anatomy. Semin Plast Surg 2015;29:158-64.

15. Saonanon P. Update on Asian eyelid anatomy and clinical relevance. Curr Opin Ophthalmol 2014;25:436-42.

16. Ezra DG, Beaconsfield M, Collin R. Surgical anatomy of the upper eyelid: Old controversies, new concepts. Exp Rev Ophthalmol 2009;1:47-57.

17. Jeong S, Lemke BN, Dortzbach RK, Park YG, Kang HK. The Asian upper eyelid: An anatomical study with comparison to the Caucasian eyelid. Arch Ophthalmol 1999;117:907-12.

18. Goldberg RA, Wu JC, Jesmanowicz A, Hyde JS. Eyelid anatomy revisited. Dynamic high-resolution magnetic resonance images of Whitnall's ligament and upper eyelid structures with the use of a surface coil. Arch Ophthalmol 1992;110:1598-600.

19. Ettl A, Daxer A, Priglinger S, Kramer J, Koornneef L. Dynamic magnetic resonance imaging of the levator palpebrae superioris muscle. Ophthalmic Res 1998;30:54-8.

20. Pillen S, van Alfen N. Skeletal muscle ultrasound. Neurol Res 2011;33:1016-24.

21. Reid RR, Said HK, Yu M, Haines GK 3rd, Few JW. Revisiting upper eyelid anatomy: Introduction of the septal extension. Plast Reconstr Surg 2006;117:65-6.

22. Callahan MA, Beard C. Anatomy. In: Callahan MC, Beard C, editor. Beard's Ptosis. 4th ed. Birmingham, AL: Aesculapius Publisher; 1990. p. 22-37.

23. Hwang K, Huan F, Kim DJ, Hwang SH. Size of the superior palpebral involuntary muscle (Müller muscle). J Craniofac Surg 2010;21:1626-9.

24. Kakizaki H, Ikeda H, Nakano T, Selva D, Leibovitch I. Junctional variations of the levator palpebrae superioris muscle, the levator aponeurosis, and Müller muscle in Asian upper eyelid. Ophthal Plast Reconstr Surg 2011;27:380-3.

25. Lyness RW, Collin JR, Alexander RA, Garner A. Histological appearances of the levator palpebrae superioris muscle in the Marcus Gunn phenomenon. Br J Ophthalmol 1988;72:104-9.

26. Strømme P, Sandboe F. Blepharophimosis-ptosis-epicanthus inversus syndrome (BPES). Acta Ophthalmol Scand 1996;74:45-7.